Check for updates

The Effect of A1 Segment Dominance on Angular Morphology of the Anterior Communicating Artery Bifurcation in Healthy and Aneurysmal Patients

Jeffrey M. Breton, Ryan Mulligan, Kaeden E. Freston, Emal Lesha, Gabrielle R. Seyouri, Alexandra Lauric, Adel M. Malek

BACKGROUND: **The anterior communicating artery (ACOM) bifurcation, a common site for aneurysm formation, carries high risk of aneurysm rupture. Due to its anastomotic nature, it exhibits complex hemodynamic and morphological profiles. Previously, ACOM angles were evaluated without accounting for unique characteristics. We evaluate ACOM angular morphology bilaterally, based on A1 trunk dominance (size and angiographic presentation), in aneurysmal and healthy patients.**

METHODS: **Bilateral catheter 3D rotational angiographic studies were available from 67 patients with ACOM aneurysms and 54 nonaneurysmal controls (242 samples total). A1 segments were classified as dominant, codominant, or nondominant based on relative diameter. Angle between ACOM and A2 segment (AcomA2) and angle between A1 and A2 segments (A1A2) angles were measured on 2D cut planes. Matched-pair analysis was performed on aneurysmal and nonaneurysmal patients with dominant/nondominant segment labels.**

RESULTS: **Aneurysms occurred on dominant (70.1%) or codominant A1 segments. A1A2 angles were significantly wider in aneurysmal bifurcations (74.1 $\pm$ 21.75°) than contralateral (53.88 $\pm$ 21.59°, $P < 0.001$) and nonaneurysmal controls (42.44 $\pm$ 14.43°, $P < 0.001$), with a threshold of 59.2° (area under the curve = 0.88). AcomA2 angle could not be evaluated in 90 volumes (37.2%) due to poor angiographic visibility of the ACOM. In unilateral and matched-pair analysis, A1A2 was significantly wider in dominant control bifurcations than nondominant sides (45.85 $\pm$ 9.83° vs. 34.47 $\pm$ 12.21°, $P = 0.003$).**

CONCLUSIONS: **ACOM angular morphology is strongly determined by A1 dominance, independent of aneurysm presence. Unlike the AcomA2 angle, A1A2 was measurable in all samples and reliably captured bifurcation angulation. ACOM bifurcations, unlike other bifurcations, require bilateral morphological and hemodynamic evaluation of the full ACOM complex. These findings inform future evaluation and modeling of cerebral vascular architecture.**

INTRODUCTION

Research suggests a strong link between altered hemodynamics at arterial bifurcation apices and intracranial bifurcation aneurysm formation.[1,2] The hemodynamic environment at bifurcations depends on morphology, and prior studies have shown that wider bifurcation angles create hemodynamic conditions conducive to aneurysm formation, such as high wall shear stress (WSS) and spatial WSS gradients.[3,4] Specifically, middle cerebral artery (MCA)[3,5] and basilar artery (BA)[4] bifurcations with aneurysms have significantly wider angles than healthy controls. MCA and BA bifurcations follow tree-like morphologies consistent with the vascular optimality principle,[3,6,7] allowing for straightforward hemodynamic and morphological analysis.

Key words
- ACOM aneurysms
- Aneurysm presence
- Intracranial aneurysms
- Vessel morphology

Abbreviations and Acronyms
A1A2: Angle between A1 and A2 segment
ACA: Anterior cerebral artery
ACOM: Anterior communicating artery
AcomA2: Angle between ACOM and A2 segment
BA: Basilar artery
CFD: Computational fluid dynamics
MCA: Middle cerebral artery
WSS: Wall shear stress

Cerebrovascular Hemodynamics Laboratory, Department of Neurosurgery, Tufts Medical Center and Tufts University School of Medicine, Boston, Massachusetts, USA

To whom correspondence should be addressed: Adel M. Malek, M.D., Ph.D. [E-mail: amalek@tuftsmedicalcenter.org]

Citation: World Neurosurg. (2025) 202:124359. http://doi.org/10.1016/j.wneu.2025.124359

*Journal homepage: **www.journals.elsevier.com/world-neurosurgery***

*Available online: **www.sciencedirect.com***

1878-8750/© 2025 The Author(s). Published by Elsevier Inc. This is an open access article under the CC BY license (http://creativecommons.org/licenses/by/4.0/).

In contrast, the circle of Willis is hemodynamically and morphologically distinct due to its compact and highly anastomotic design.[7,8] It acts as a safeguard, compensating for reduced flow in certain brain areas, leading to complex hemodynamic dependencies that are not fully understood. This complexity raises methodological questions regarding how best to assess the anterior communicating artery (ACOM) complex.[9] The ACOM, forming the circle of Willis's anterior link, is the most common site of intracranial aneurysms and has a high rupture rate,[10] accounting for ~20% of subarachnoid hemorrhage cases, a condition still associated with high mortality and morbidity despite treatment advances.

Previous research often evaluated the ACOM bifurcation unilaterally,[11-13] ignoring the likely morphological and hemodynamic interdependence between the two anterior cerebral arteries (ACAs). Conversely, other studies assessed bilateral aneurysmal ACOM bifurcations but omitted trunk dominance,[14,15] an integral morphological feature of the ACOM complex.

In contrast to previous work, we propose that a bilateral, integrated approach offers the most complete characterization of this compact, hemodynamically unique site. Unlike earlier studies,[14-17] we evaluate ACOM bifurcations bilaterally in both aneurysmal and healthy patients. Given that trunk dominance is key to ACOM morphology, and ACOM aneurysm presence is linked to ACA trunk dominance,[18] we specifically selected healthy controls with similar morphology. This allows us to determine whether ACOM morphology is more dependent on trunk dominance or aneurysm presence.

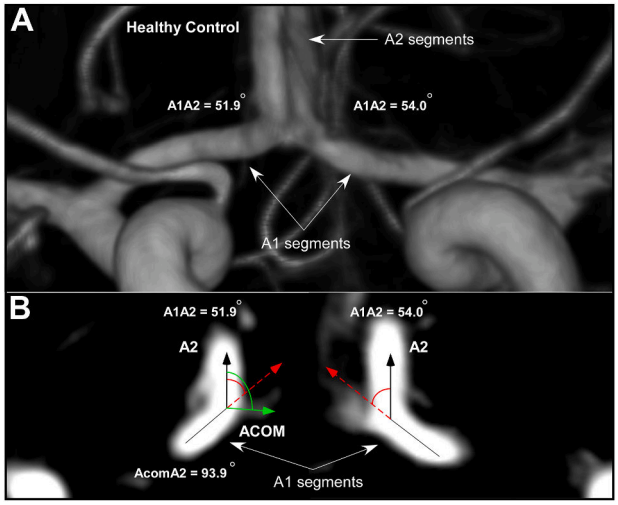


Figure 1. Angle between A1 and A2 segments (A1A2) and angle between ACOM and A2 segment (AcomA2) angle measurement. (**A**) 3D volume-rendered angiographic data for a healthy patient showing bilateral anterior cerebral arteries. Both A1 segments have been labeled as codominant based on size and angiographic presentation. (**B**) Illustration of measurement methodology. A1A2 and AcomA2 angles are shown on multiplanar reconstruction planes through the center of the vessels, following flow direction measuring conventions. The anterior communicating artery (ACOM) bifurcation is sufficiently visible to determine the location of the bifurcation, but it does not permit reliable bilateral measurement of the AcomA2 angle due to insufficient vessel definition.

MATERIALS AND METHODS

Patient Selection

Three-dimensional volumetric data were collected between 2009 and 2024 from patients presenting with unilateral intracranial aneurysm at the ACOM bifurcation, for whom both left and right internal carotid cerebral angiograms were available. Patients with A1 segment hypoplasia were excluded from the study. In addition, bilateral angiographic data were analyzed from healthy individuals who had undergone cerebral angiography for other reasons (excluding family history of intracranial aneurysm). Demographic information was retrieved from a prospectively compiled database.

This research was approved by the Institutional Review Board ethics committee. Patient consent was waived due to the retrospective nature of the study not impacting patient clinical care.

Cerebral Angiography and Data Processing

Three-dimensional cerebral angiograms were collected using Siemens Artis (Malvern, PA) biplane angiographic systems and reconstructed using the Leonardo clinical software packages from the manufacturer. Volumes were processed and analyzed using Amira visualization software platform version 5.3.3 (Thermo Fisher Scientific, Waltham, MA).

A1 Dominance

The A1 segments of the ACA were labeled by the senior authors as dominant, codominant, and nondominant based on size and angiographic presentation. In patients with ACOM aneurysms, the aneurysmal A1 (left/right) was selected as the side which provided complete filling of the aneurysm on ipsilateral injection.

Morphological Feature Extraction

Two angle measurements were evaluated in this study: 1) the angle between A1 and A2 segments (A1A2) angle, formed by the A1 and corresponding A2 segment, and 2) the Angle between ACOM and A2 segment (AcomA2) angle, formed by the A2 segment and the ACOM (Figure 1). Measurements were performed as described in the literature[3,4,19] by a trained imaging scientist and validated by a second blinded operator (mean operator difference 6.68°, standard deviation 9.47°, coefficient of variation 7.93%), using scientific imaging software Amira 5.3 (FEI, Hillsboro, OR). Angles were measured in the direction of flow (Figure 1B), following the convention set by Rossitti and Lofgren.[6] Thus, angles represent deviation from the parent vessel's flow direction.[3,6,7] Unlike recent studies,[11-13] this convention aligns with seminal research evaluating angular deviations at aneurysmal bifurcations.[6,7] Specifically, vessel centerlines were generated in Amira, and multiplanar reconstruction through the volume was performed at the site of ACOM, using local centerlines as guidelines for plane fitting (Figure 1B). Accordingly, measurement was performed on 2-dimensional cut-planes fitted for most accurate evaluation. ACOM angle measurements were excluded when the artery's course could not be confidently visualized angiographically. The ACOM's short length and variable contrast

Table 1. Univariate Statistical Analysis of the Angular Morphology of the Anterior Communicating Artery Bifurcation, Comparing the Aneurysmal, Contralateral, and Healthy Patients in Which Contralateral A1 Segments are Labeled as Dominant, Nondominant, and Codominant, Respectively

All Samples	Aneurysmal (An) N = 67	Contralateral (C) N = 67	Healthy Dominant (Hd) N = 19	Healthy Nondominant (Hn) N = 19	Healthy Codominant (Hc) N = 70
Age (years)	56.02 ± 11.30	56.02 ± 11.30	52.36 ± 16.14	52.36 ± 16.14	53.96 ± 13.63
	An versus *C* $P = 1.00$	*C* versus *Hn* $P = 0.25$	*An* versus *Hd* $P = 0.27$	*Hd* versus *Hn* $P = 1.00$	*C* versus *Hc* $P = 0.31$
A1A2 (°)	74.14 ± 21.75	53.88 ± 21.59	45.85 ± 9.83	34.47 ± 12.21	43.70 ± 14.96
	An versus *C* $P < 0.001$*	*C* versus *Hn* $P < 0.001$*	*An* versus *Hd* $P < 0.001$*	*Hd* versus *Hn* $P = 0.003$	*C* versus *Hc* $P = 0.002$*
All Samples	**Aneurysmal (An) (N = 56)**	**Contralateral (C) (N = 20)**	**Healthy Dominant (Hd) (N = 18)**	**Healthy Nondominant (Hn) (N = 3)**	**Healthy Codominant (Hc) (N = 51)**
AcomA2 (°)	136.31 ± 21.98	107.33 ± 18.64	103.36 ± 18.54	96.1 ± 12.74	103.74 ± 20.41
	An versus *C* $P < 0.001$*	*C* versus *Hn* $P = 0.37$	*An* versus *Hd* $P < 0.001$*	*Hd* versus *Hn* $P = 0.57$	*C* versus *Hc* $P = 0.51$

Shown is mean and standard deviation.
A1A2° was measured at the ACOM bifurcation as the angle formed by the A2 segment with the extension of the A1 segment. AcomA2° was measured at the ACOM bifurcation as the angle formed by the ACOM and the A2 segment.
AcomA2, angle between ACOM and A2 segment; A1A2, angle between A1 and A2 segments.
*Indicates statistical significance (assumed for $P < 0.05$).

filling contribute to substantial evaluation variability and measurement challenges.

Patient-Derived Models

Two representative patient-specific models, one aneurysmal and one healthy patient, were selected for computational fluid dynamics (CFD) analysis. Following vessel segmentation in Amira, the aneurysms were digitally removed by local Laplacian smoothing,[20] and the parent vessels were reconstructed in MeshLab version 2023.12 (ISTI-CNR, Pisa, Italy). Similar to Castro et al.,[21] segmented vascular models of the left and right sides of the arterial trees were merged after applying rigid manual transformation using SpaceClaim 2022R1 (Ansys Inc., Labanon, NH), allowing for bilateral modeling of the ACOM bifurcation.

CFD

CFD simulations were performed using Fluent 2022R1 (Ansys Inc.), by modeling steady state laminar flow with a Carreau non-Newtonian profile to better approximate the viscosity and flow of blood.[22] In order to account for morphological variations in vessel size, shape and length, flow scaling factors were determined for each model to insure ideal parent vessel WSS conditions of approximately 1.5 Pa at the internal carotid arteries (measured on diameter proximal from the internal carotid bifurcation). Subsequently, steady flow was applied at the inlet according to the resulting scaled velocity, with 0 gauge pressure at the outlets.

Postprocessing analysis was performed using EnSight 2021R1 (Ansys Inc.), allowing for evaluation and visualization of WSS and velocity at the ACOM bifurcation.

Statistical Analysis

Data were analyzed using JMP version 17.2 (SAS Institute, Cary, NC) assuming a significance threshold of $P < 0.05$. Angle parameters were tested independently using student t-test analysis to determine discriminating factors between aneurysmal and control ACOM bifurcations. In addition, bilateral angle analysis was performed using matched-pair analysis for both aneurysmal and healthy groups.

RESULTS

Patient Demographics

Three hundred twelve 3D rotational angiographic datasets from 156 patients were available. Exclusion criteria were variant anatomy, poor image quality, and absence of bilateral data. Consequently, 67 patients with ACOM aneurysms (44 females; average age 56.02 ± 11.30 years) and 54 healthy, nonaneurysmal patients (26 females; average age 53.5 ± 14.6 years) were included. Bilateral angiograms were available in both groups, yielding 242 angiographic volumes (67 aneurysmal, 67 nonaneurysmal contralaterals, and 108 controls). There was no significant age difference between aneurysmal and control patients (Table 1). Sixteen ACOM aneurysms were ruptured. None of the ruptured aneurysms had intracerebral hematoma, which could have complicated angle evaluation and altered measurements.

A1 Dominance

Presence of intracranial aneurysm at the ACOM bifurcation was previously associated with ACA trunk dominance.[23] In this study, 47 (70.1%) of the 67 aneurysmal volumes were labeled as having a dominant A1 segment on the aneurysm side; the remainder were labeled codominant. Conversely, contralateral nonaneurysmal sides were labeled nondominant in 47 volumes and codominant in 20, with no sides labeled dominant. Eleven ruptured aneurysms (68.7% of ruptured) had a dominant A1 segment on the aneurysm side.

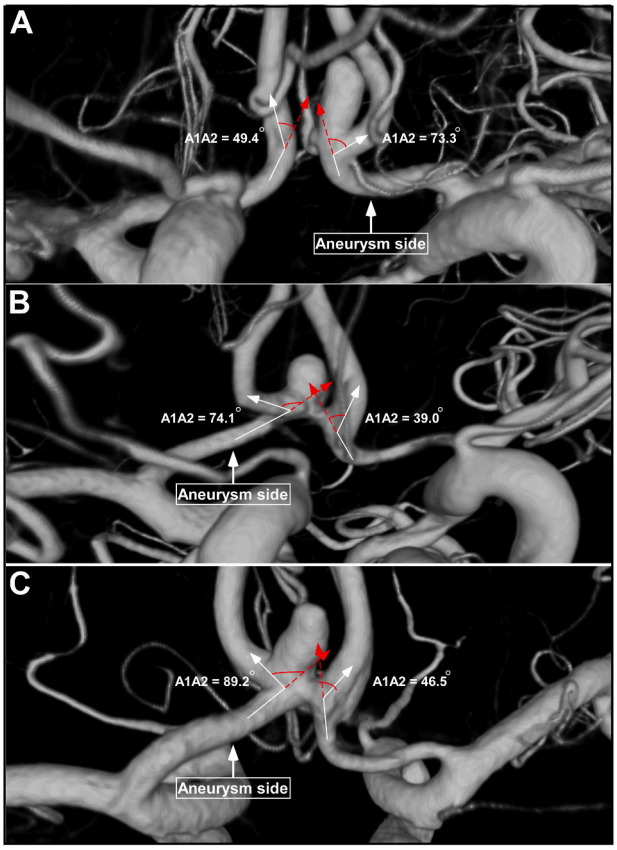


Figure 2. Aneurysmal data. (**A**–**C**) 3D volume of bilateral angiographic data from patients with anterior communicating artery (ACOM) aneurysms. A1 segments were labeled as dominant, codominant, and nondominant based on size and angiographic presentation. Aneurysm occurs most often on dominant and codominant segments. Aneurysmal angle between A1 and A2 segments (A1A2) angles are significantly larger. Due to limited ACOM visibility, angle between ACOM and A2 segment (AcomA2) angles were unmeasurable in 12.5% of aneurysmal and 65.6% of contralateral volumes. Note that for accurate evaluation, all measurements were performed on 2D planes as described. Angle overlay shown for illustration only.

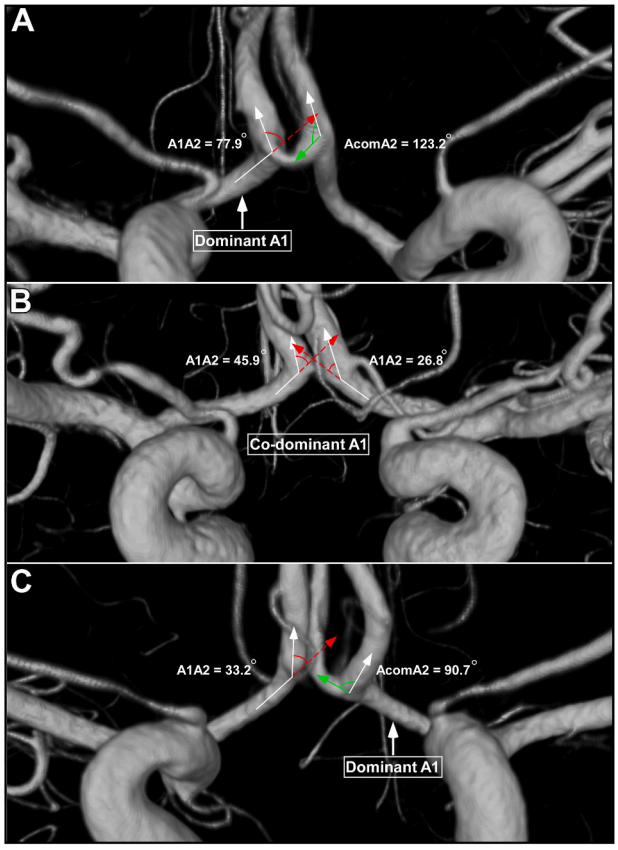


Figure 3. Healthy data. (**A**–**C**) 3D volume of bilateral angiographic data from healthy controls. A1 segments were labeled as dominant, codominant, and nondominant based on size and angiographic presentation. As with aneurysmal patients, angle between A1 and A2 segments (A1A2) angles are significantly wider on the dominant side. Angle between ACOM and A2 segment (AcomA2) angles could not be evaluated on 32.7% of healthy volumes due to limited opacification and anatomical variability. Note that for accurate evaluation, all measurements were performed on 2D planes as described. Angle overlay shown for illustration only.

Among healthy controls, 35.2% of volumes were labeled dominant/nondominant, while 64.8% were labeled codominant.

AcomA2 Angles

Similar to measurement of MCA[3] and BA[4] bifurcation angles, we aimed to evaluate the direct ACOM bifurcation angle, namely the AcomA2 angle. In 37.2% of cases (90 volumes), the ACOM was insufficiently visualized for reliable angle determination, primarily due to weak contrast filling and anatomical constraints. This was the case for 9 aneurysmal volumes (13.4% of aneurysms), 45 volumes contralateral to aneurysmal sides (67.1% for contralateral), and 36 healthy volumes (33.4% of controls).

Figure 1B shows a healthy patient in which ACOM is not sufficiently defined on angiographic images for confident bilateral evaluation. Whereas the position of the ACOM bifurcation is defined, the ACOM vessel cannot be properly evaluated for angular measurement. This situation is characteristic of volumes classified as codominant or nondominant and was previously described.[24] To the extent that it could be evaluated, AcomA2 angles were significantly larger in aneurysmal volumes compared to both contralateral (136.31 ± 21.98° vs. 107.33 ± 18.64°, $P < 0.001$) (Table 1) and all healthy controls (136.31 ± 21.98° vs. 103.32 ± 19.55°, $P < 0.001$).

A1A2 Angles

In contrast to AcomA2 angle, the A1A2 angle was straightforward to measure as shown in Figure 1B and detailed in Table 1. Figures 2 and 3 show A1A2 measurements on aneurysmal and healthy patients, respectively.

Statistically (Figure 4), the aneurysmal A1A2 angle was significantly larger than the corresponding contralaterals

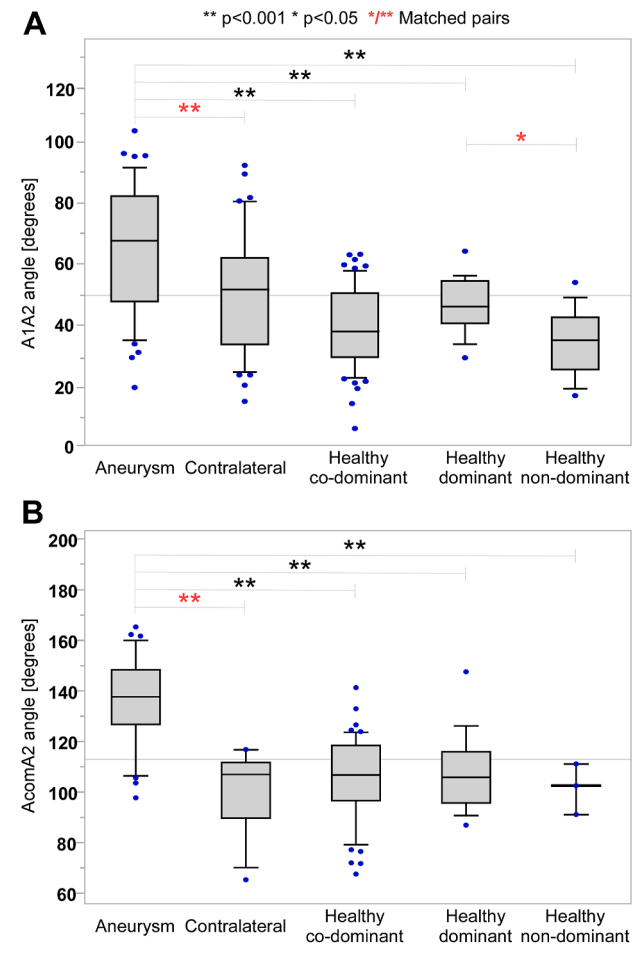


Figure 4. Box plot visualization of angular measurements across patient groups. (**A**) Angle between A1 and A2 segments (A1A2) angle comparison. (**B**) Angle between ACOM and A2 segment (AcomA2) angles comparison. Statistical significance was assumed for $P < 0.05$. The aneurysmal samples had significantly wider A1A2 and AcomA2 angles compared to contralateral and healthy volumes. The dominant A1 segment corresponds to wider A1A2 angles across all cohorts. ** represents P value < 0.001, * represents P value < 0.05. Red ** represents statistical significance in both univariate and matched pair analysis.

Table 2. Matched-Pair Statistical Analysis of the Angular Morphology of the Anterior Communicating Artery Bifurcation, Comparing the Aneurysmal Samples with Their Corresponding Contralateral and Healthy Patients in Which Contralateral A1 Segments are Labeled as Dominant and Nondominant, Respectively

Bilateral samples	Aneurysmal (An) N = 67	Contralateral (C) N = 67
A1A2 (°)	74.14 ± 21.75	53.88 ± 21.59
		An versus *C* *P* < 0.001*
AcomA2 (°) (21 pairs with visible ACOM)	143.49 ± 16.84	107.04 ± 20.28
		An versus *C* *P* < 0.001*
	Healthy dominant (Hd) N = 19	**Healthy nondominant (Hn) N = 19**
A1A2 (°)	45.85 ± 9.83	34.47 ± 12.21
		Hd versus *Hn* *P* = 0.007*
AcomA2 (°) (3 pairs with visible ACOM)	102.10 ± 18.47	91.86 ± 14.17
		Hd versus *Hn* *P* = NA

Shown is mean and standard deviation.
A1A2° was measured at the ACOM bifurcation as the angle formed by the A2 segment with the extension of the A1 segment. AcomA2° was measured at the ACOM bifurcation as the angle formed by the ACOM and the A2 segment.
AcomA2, angle between ACOM and A2 segment; A1A2, angle between A1 and A2 segments.
*Indicates statistical significance (assumed for $P < 0.05$).

(74.14 ± 21.75° vs. 53.88 ± 21.59°, P < 0.001) and all healthy groups (74.14 ± 21.75° vs. 42.44 ± 14.43°, P < 0.001) regardless of dominance label. An A1A2 angle threshold of 59.2° was established to discriminate between aneurysmal samples and healthy dominant samples (area under the curve = 0.88, specificity 79.8%, sensitivity 88.8%). In addition, the contralateral group had A1A2 angles significantly larger compared to all healthy controls (53.88 ± 21.59° vs. 42.44 ± 14.43°, P = 0.002). Within healthy subgroups, nonaneurysmal contralaterals had significantly wider A1A2 angles compared to healthy nondominant (P = 0.004) and healthy codominant (P = 0.01) bifurcations but were not different from healthy dominant sides (P = 0.16). The analysis was repeated after exclusion of ruptured samples and resulted in similar statistical results.

In healthy controls, dominant bifurcations had significantly wider A1A2 angles compared to the nondominant sides (45.85 ± 9.83° vs. 34.47 ± 12.21°, P = 0.003). Codominant bifurcations had significantly wider A1A2 angles compared to nondominant sides (P = 0.02) but were not different from dominant sides (P = 0.55). AcomA2 angles were not statistically different between healthy subgroups.

Matched Pair Analysis

Matched pair analysis was performed for the aneurysmal group (aneurysmal vs. contralateral) as well as for the healthy patients in which one side was labeled as dominant and the other side was labeled as nondominant (dominant vs. nondominant). Matched pair analysis allows for evaluations in which each patient acts as its own control, removing possible dependency on age, gender, and clinical characteristics.

Bilateral analysis confirmed univariate analysis with aneurysmal bifurcations having significant wider A1A2 (P < 0.001) and AcomA2 (P < 0.001) angles compared to corresponding contralaterals (Tables 2). Healthy dominant bifurcations had

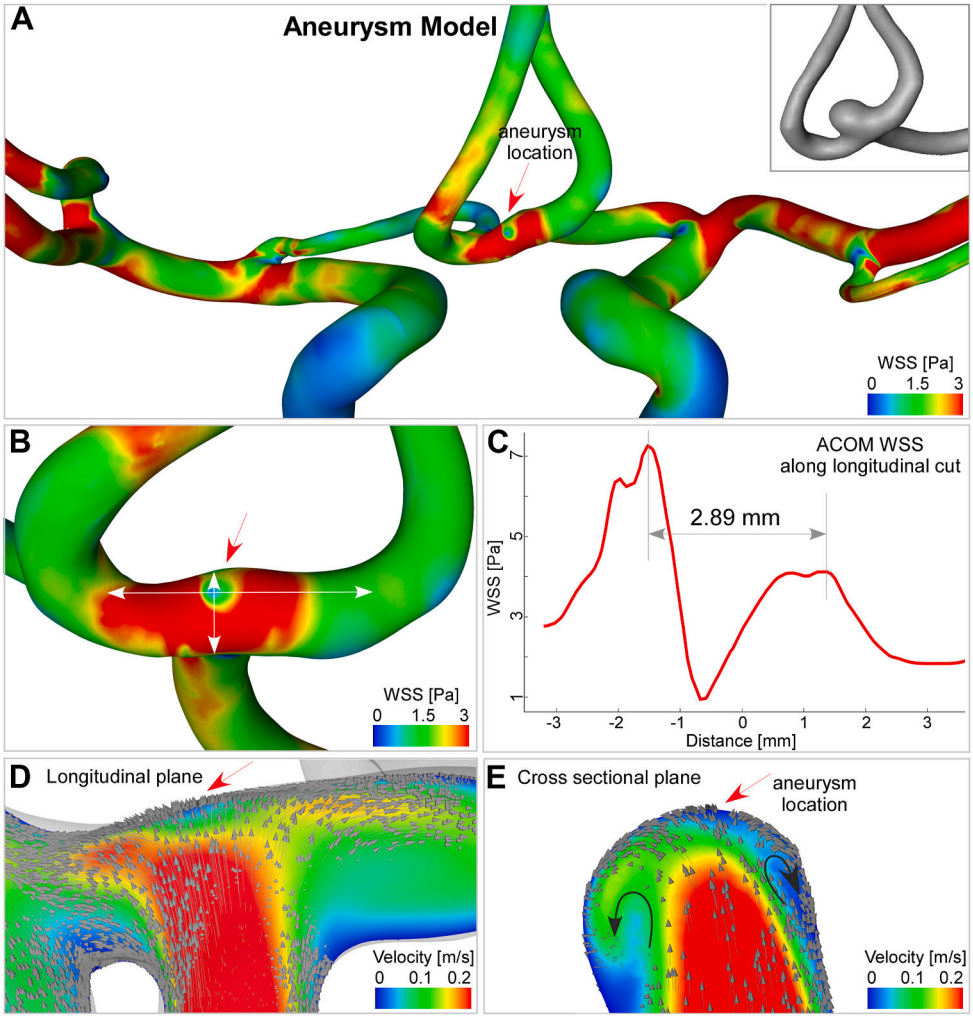


Figure 5. Computational fluid dynamics on an aneurysmal patient (aneurysm digitally removed). (**A**) Wall shear stress (WSS) distribution across the model, with the original model show in the inset. *Arrow* points to the location of the aneurysm. (**B**) Detail of WSS at anterior communicating artery (ACOM). Arrows show the direction and position of longitudinal and cross sectional planes. (**C**) WSS line plotting in the longitudinal plane. The location of the aneurysm is flanked by high WSS peaks. The distance between WSS peaks is 2.89 mm. (**D**) Detail of velocity vector field in the longitudinal cut. There is jet impingement at the aneurysm location. The *arrow* shows the aneurysm location. (**E**) Detail of velocity field in the cross sectional cut showing flow separation at the bifurcation apex and the formation of two vortices indicative of high rotational WSS and gradients. *Arrows* show vortex direction.

significantly wider A1A2 ($P = 0.007$) angles, compared to corresponding nondominant bifurcations. AcomA2 statistics could not be evaluated in this group due to small sample as only 3 pairs of healthy dominant/nondominant bifurcations had bilateral AcomA2 measurement.

A1A2 Angle Dependency on Age, Gender, and Aneurysm Size

A weak correlation was detected between age and A1A2 angle in aneurysmal samples only ($P = 0.007$, $R^2 = 0.11$). There was no statistical correlation between age and angle AcomA2 for any of the groups. Angle AcomA2 was statistically larger in healthy male compared to healthy female bifurcations ($108.93 \pm 13.95°$ vs. $98.58 \pm 22.36°$, $P = 0.02$). No similar effect was detected for A1A2 angle.

The average size of the aneurysms in this study was 5.24 ± 2.80 mm, with a mean neck width of 3.61 ± 1.41. There was no correlation between angles A1A2, AcomA2, and the aneurysm size.

Angle A1A2 was positively correlated with aneurysm neck width ($P = 0.01$, $R^2 = 0.10$), whereas angle AcomA2 was not ($P = 0.24$). Analysis was repeated after exclusion of aneurysms with a neck size larger than 5 mm (10 aneurysms). No statistical correlation was observed between neck size and angles A1A2 ($P = 0.13$) and

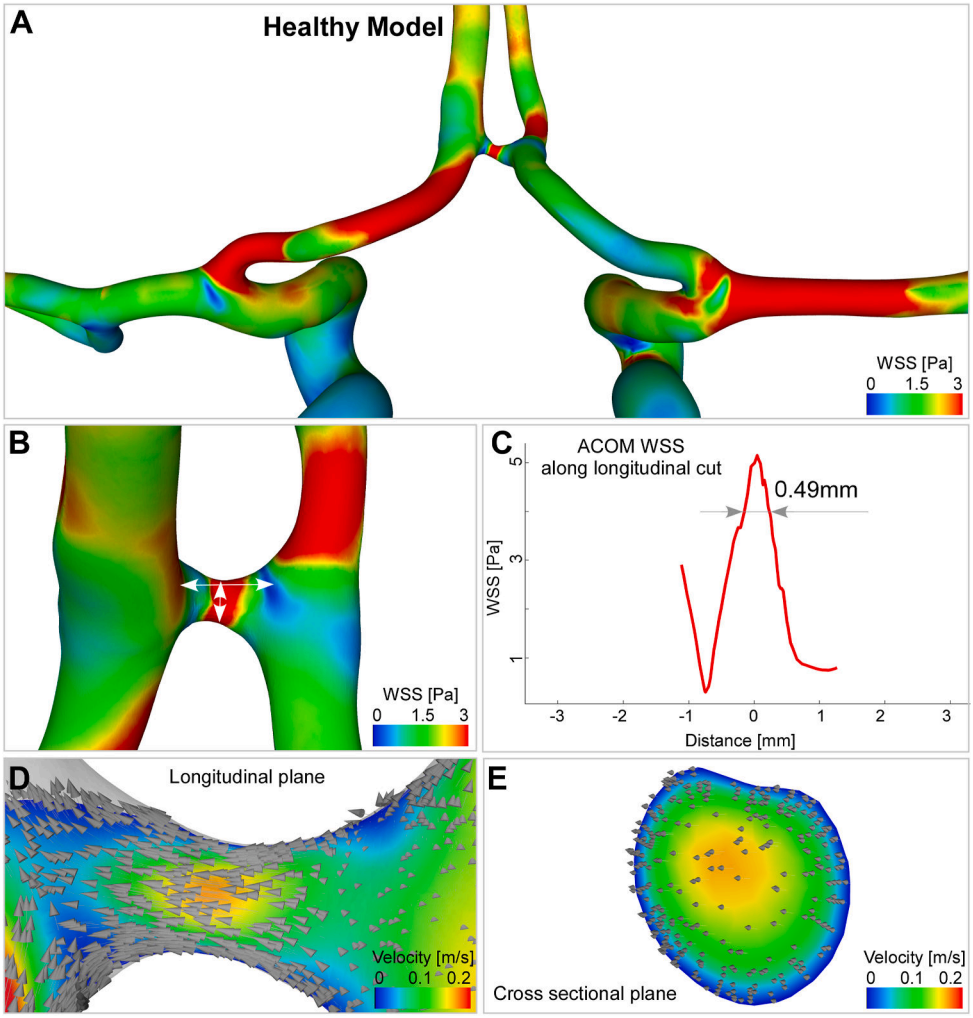


Figure 6. Computational fluid dynamics on a healthy control. (**A**) Wall shear stress (WSS) on the entire model. (**B**) Detail of WSS at anterior communicating artery (ACOM) showing a much localized region of higher WSS. *Arrows* show the direction and position of longitudinal and cross sectional planes. (**C**) WSS line plotting in the longitudinal plane. The distance span by WSS >4 Pa is only 0.49 mm. (**D**) Detail of velocity vector field in the longitudinal cut. (**E**) Detail of velocity field in the cross sectional cut showing evenly distributed flow, suggestive of stable hemodynamics.

AcomA2 ($P = 0.41$) for the group of 57 remaining aneurysms. In addition, angle analysis was repeated after exclusion of aneurysms with wide neck size (>5 mm) to determine the effect of neck size on angle statistics. In this remaining group of 57 aneurysms, angles A1A2 and AcomA2 were significantly wider compared to both contralateral and healthy controls.

CFD

CFD simulations were conducted on representative aneurysmal (aneurysm digitally removed) and healthy models to evaluate the hemodynamics at the ACOM bifurcation and determine differences that could create conditions for aneurysm origination (Figures 5 and 6).

WSS maps in the aneurysmal model show high-stress regions at the location of the aneurysm neck and along the wall of the ACOM, corresponding to the impingement by dominant A1 flow, as evident in the velocity patterns on the longitudinal and cross-sectional planes (Figure 5). The impingement area corresponds to the aneurysm location. Velocity patterns reveal high-velocity jets at the apex which dissipate sharply along the vessel wall creating conditions for directional instability, vortex formation, and high rotational WSS[25] as evident in the cross-sectional velocity detail (Figure 5E). Plotting WSS values along a longitudinal cut, spanning the ACOM and covering the aneurysm location, reveal high WSS peaks of 7.27 Pa and 4.12 Pa flanking the area of impingement. The distance between WSS peaks was evaluated at 2.89

mm. This is consistent with previously reported results[25] showing a widening of the region of flow separation and vortex formation at increased angles, characterized by high transverse rotational shear stress and gradients.

In contrast, WSS maps on the healthy model show a much localized area of high WSS with a peak of 5.15 Pa (**Figure 6**). Plotting WSS along a longitudinal cut, spanning the length of ACOM, shows that only 0.49 mm of the ACOM is subjected to WSS values higher than 4 Pa. Velocity patterns reveal velocity vectors were more evenly distributed, suggesting stable and balanced hemodynamic conditions.

DISCUSSION

The ACOM is a common site for aneurysm formation with more than one fourth of all cerebral aneurysms occurring at this location. These aneurysms have a high incidence of rupture of approximately 30%,[10] often at relatively small sizes.[26-28] Because of the morphological and hemodynamic complexity of the ACOM bifurcation, ACOM aneurysms can present some challenges to treat and manage clinically. These characteristics make the study of the anterior communicating artery complex, and the understanding of the underlying mechanisms for ACOM aneurysm origination and progression, particularly relevant.

Given their frequent occurrence on A1 dominant segments, ACOM aneurysms might be mistakenly modeled as tree-like bifurcations, similar to those seen in MCA and BA systems. However, hemodynamic modeling of this location[29] does not support such an approach and suggests that the ACOM complex needs to be evaluated taking into account bilateral inflow features.

This study evaluates the morphology of the ACOM bifurcation bilaterally and introduces a new dimension by establishing a morphological codependence on A1 trunk dominance within the ACOM complex. Unlike prior studies,[14-17,23] which primarily focused on unilateral or aneurysmal anatomy, we apply a bilateral analysis stratified by A1 dominance to both aneurysmal and nonaneurysmal patients. This allows us to distinguish anatomical variation inherent to vascular dominance from changes associated with aneurysm formation.

In contrast to measurement of MCA[3] or BA[4] bifurcations, in which the bifurcation angulation can be evaluated as the angle between daughter vessels, our results confirm that the AcomA2 angle could not be evaluated in 37.2% of cases due to the ACOM's small size and inconsistent contrast opacification, limiting its utility for comprehensive bilateral analysis. This is consistent with reports on angiographic imaging of the ACOM[24] and supported by hemodynamic studies[29] which show that the ACOM is characterized by dynamic cross-flow which explains its weak contrast filling in codominant and nondominant configurations. In contrast to AcomA2 angle which could not be evaluated in one-third of the samples, A1A2 angle was accurately measured in all samples. Our results show A1A2 angle as a reliable descriptor of the ACOM bifurcation angular morphology which allows for comparison with contralateral or healthy sample.

Although previous studies[14-17] evaluate the direct angle between A1 and A2 segments, we report the angle as the deviation from the direction of flow in the parent vessel.[3,6,7] This is the convention set by Rossitti and Lofgren[6] as the preferred way to evaluate the vascular optimality at bifurcations. Consequently, we report that the A1A2 angle is significantly larger in aneurysmal bifurcations compared with both of their corresponding contralateral and healthy controls. Importantly, given the unique morphology of the circle of Willis, we report that A1A2 angle is significantly larger on the A1 dominant side, regardless of aneurysm presence. This strongly suggests a morphological and hemodynamic interdependence between the two A1 segments as they form the anterior link of the circle of Willis. These findings show that the hemodynamic modeling of the ACOM bifurcations and aneurysms needs to be performed bilaterally by considering inflow contributions from both A1 segments. This is despite the fact that most aneurysms are filled unilaterally.[18] Modeling the ACOM bifurcations as a tree structure misses the unstable flow characteristics of the ACOM[24] and can result in less accurate hemodynamic evaluations.

It was suggested that arterial bifurcations follow the vascular optimality principle which enforces minimal energy expenditure and loss at bifurcations and dictates the caliber and angular relationships between parent and daughter vessels. It was shown that bifurcations outside the circle of Willis[7,30] closely follow the optimality principle, whereas those within the circle of Willis do not.[7] Whereas recent studies[12] have attempted to evaluate the optimality principle as it applies to the ACOM bifurcation, our results caution against treating the ACOM as a daughter vessel of the A1 segment when attempting to evaluate the optimality principle as it applies to the ACOM bifurcation. As mentioned, the ACOM has a unique anatomical function in the brain, associated with hemodynamic patterns that predict a confluence of hemodynamic forces in the distribution of energy within the circle of Willis, in contrast to other bifurcations configurations such as the MCA.

It was previously suggested that aneurysm formation occur at regions subject to high WSS particularly when combined with flow impingement.[31] In addition, previous studies have suggested that the apex of a vascular bifurcation may be shielded from hemodynamic stress by a narrow band of densely packed collagen fibers which typically ranges from 0.42 mm^2 to 1.40 mm^2.[32,33] This band covers the medial pad and contributes to the region's strength and stiffness. Animal experiments using surgically constructed arterial bifurcations revealed that, in contrast, the area adjacent to the medial pad exhibited disrupted internal elastic lamina and endothelial loss, features consistent with early aneurysm development.[34] The CFD simulations suggest the wider A1A2 angles flow impingement regions that are outside the protective limits of the medial pad, exposing adjacent tissue to elevated hemodynamic stress that may promote destructive remodeling and contribute to aneurysm formation.

Overall, aneurysmal and healthy ACOM bifurcations have distinct morphology stemming from their position within the circle of Willis. Despite common characteristics, aneurysmal and healthy vasculature show important differences in their angular morphology, which provides new insights into how angle assessment might be related to a higher risk of aneurysm presence. Our study is retrospective in nature, and its clinical relevance would need to be confirmed in a prospective fashion. However, the conclusion of this study, including the identification of angle thresholds, could potentially be used to monitor and

screen patients that are asymptomatic, have a family history of aneurysms, or have been identified of being at risk for developing multiple aneurysms. The results of this study advance the understanding of the ACOM unique morphology and represent a precursor for a more in-depth evaluation of the vascular optimality at this location. While this report suggests future directions for the morphological and hemodynamic evaluation of the anterior communicating complex, more research will be needed to determine the full implications of these findings and to provide insight into clinical relevance.

Study Limitations

As with similar retrospective research, the association between bifurcation morphology and aneurysm presence suggests correlation but not causation, a limitation shared across studies. Given the retrospective nature of this work, we cannot conclude that wider A1A2 angles preceded aneurysm formation; aneurysm development may be an epiphenomenon of wider bifurcations rather than a direct consequence of high-risk morphology. Prospective analysis of MCA bifurcations[35] suggests wide branching angles precede aneurysm initiation, whereas analysis of healthy BA bifurcations indicates widening may occur with age.[4] However, no conclusive data exist to settle this issue. It remains possible that aneurysm formation could alter bifurcation morphology. Notably, smaller aneurysms and those with small necks occurred at wide bifurcations in this study, arguing against significant angle alteration after aneurysm formation.

Given the primary focus of this study, only representative CFD simulations were performed to illustrate potential hemodynamic implications of observed angular differences. These simulations used standardized inlet conditions, as patient-specific flow data were not available from the 3D rotational angiograms. This approach is common in retrospective CFD studies, where anatomical geometries are available but individualized hemodynamic measurements are not. Future work will require larger cohorts and incorporation of patient-specific inflow waveforms to better characterize the interplay between morphological variation and flow dynamics.

CONCLUSION

This study evaluates ACOM angular morphology (AcomA2 and A1A2 angles) bilaterally based on A1 trunk dominance, both in aneurysmal and also in healthy patients. AcomA2 angle could not be evaluated in a third of our samples proposing that A1A2 is a more reliable measure in evaluating the ACOM bifurcation morphology. Matched pair analysis shows that ACOM bifurcation angles strongly depend on A1 dominance, independent of aneurysm presence. In contrast to other locations, morphological and hemodynamic evaluation of the ACOM bifurcation cannot be performed unilaterally and needs to consider the entire anterior communicating complex. CFD simulations confirm these findings and suggest that wider A1A2 angles results in high-impingement zone of elevated hemodynamic stress that may promote destructive vessel remodeling and contribute to aneurysm formation. These findings have implications for future evaluations and modeling of this key part of the brain's vascular system.

CRediT AUTHORSHIP CONTRIBUTION STATEMENT

Jeffrey M. Breton: Data curation, Formal analysis, Writing — original draft. **Ryan Mulligan:** Data curation. **Kaeden E. Freston:** Data curation, Software. **Emal Lesha:** Data curation. **Gabrielle R. Seyouri:** Data curation. **Alexandra Lauric:** Data curation, Formal analysis, Methodology, Validation, Visualization, Writing — review & editing. **Adel M. Malek:** Conceptualization, Investigation, Methodology, Supervision, Validation, Visualization, Writing — review & editing.

REFERENCES

1. Sforza DM, Putman CM, Cebral JR. Hemodynamics of cerebral aneurysms. *Ann Rev Fluid Mech*. 2009;41:91-107.
2. Meng H, Tutino VM, Xiang J, Siddiqui A. High WSS or low WSS? Complex interactions of hemodynamics with intracranial aneurysm initiation, growth, and rupture: toward a unifying hypothesis. *AJNR Am J Neuroradiol*. 2013;35:1254-1262.
3. Baharoglu MI, Lauric A, Safain MG, Hippelheuser J, Wu C, Malek AM. Widening and high inclination of the middle cerebral artery bifurcation are associated with presence of aneurysms. *Stroke*. 2014;45:2649-2655.
4. Tütüncü F, Schimansky S, Baharoglu MI, et al. Widening of the basilar bifurcation angle is associated with presence of intracranial aneurysm, age, and female gender. *J Neurosurg*. 2014;121:1401-1410.
5. Sadatomo T, Yuki K, Migita K, Imada Y, Kuwabara M, Kurisu K. Differences between middle cerebral artery bifurcations with normal anatomy and those with aneurysms. *Neurosurg Rev*. 2013;36:437-445.
6. Rossitti S, Lofgren J. Optimality principles and flow orderliness at the branching points of cerebral arteries. *Stroke*. 1993;24:1029-1032.
7. Ingebrigtsen T, Morgan MK, Faulder K, Ingebrigtsen L, Sparr T, Schirmer H. Bifurcation geometry and the presence of cerebral artery aneurysms. *J Neurosurg*. 2004;101:108-113.
8. Vrselja Z, Brkic H, Mrdenovic S, Radic R, Curic G. Function of circle of Willis. *J Cereb Blood Flow Metab*. 2014;34:578-584.
9. Ujiie H, Liepsch DW, Goetz M, Yamaguchi R, Yonetani H, Takakura K. Hemodynamic study of the anterior communicating artery. *Stroke*. 1996;27:2086-2093. ; discussion 2094.
10. Zacharia BE, Hickman ZL, Grobelny BT, et al. Epidemiology of aneurysmal subarachnoid hemorrhage. *Neurosurg Clin N Am*. 2010;21:221-233.
11. Zhang XJ, Gao BL, Hao WL, Wu SS, Zhang DH. Presence of anterior communicating artery aneurysm is associated with age, bifurcation angle, and vessel diameter. *Stroke*. 2018;49:341-347.
12. Zhang XJ, Li CH, Hao WL, Zhang DH, Gao BL. The optimality principle decreases hemodynamic stresses for aneurysm initiation at anterior cerebral artery bifurcations. *World Neurosurg*. 2018;121:e379-e388.
13. Zhang XJ, Li CH, Hao WL, Zhang DH, Ren CF, Gao BL. Enlarged anterior cerebral artery bifurcation angles may induce abnormally enhanced hemodynamic stresses to initiate aneurysms. *World Neurosurg*. 2018;120:e383-e391.
14. Kasuya H, Shimizu T, Nakaya K, Sasahara A, Hori T, Takakura K. Angles between A1 and A2 segments of the anterior cerebral artery visualized by three-dimensional computed tomographic angiography and association of anterior communicating artery aneurysms. *Neurosurgery*. 1999;45:89-93. ; discussion 93-4.
15. İdil Soylu A, Ozturk M, Akan H. Can vessel diameters, diameter ratios, and vessel angles predict the development of anterior communicating artery aneurysms: a morphological analysis. *J Clin Neurosci*. 2019;68:250-255.
16. Kaspera W, Ładziński P, Larysz P, et al. Morphological, hemodynamic, and clinical

independent risk factors for anterior communicating artery aneurysms. *Stroke*. 2014;45:2906-2911.

17. Ye J, Zheng P, Hassan M, Jiang S, Zheng J. Relationship of the angle between the A1 and A2 segments of the anterior cerebral artery with formation and rupture of anterior communicating artery aneurysm. *J Neurol Sci*. 2017;375:170-174.

18. Charbel FT, Seyfried D, Mehta B, Dujovny M, Ausman JI. Dominant A1: angiographic and clinical correlations with anterior communicating artery aneurysms. *Neurol Res*. 1991;13:253-256.

19. Rosato R, Comptdaer G, Mulligan R, et al. Increased focal internal carotid artery angulation in patients with posterior communicating artery aneurysms. *J Neurointerv Surg*. 2020;12:1142.

20. Lauric A, Hippelheuser J, Safain MG, Malek AM. Curvature effect on hemodynamic conditions at the inner bend of the carotid siphon and its relation to aneurysm formation. *J Biomech*. 2014;47:3018-3027.

21. Castro MA, Putman CM, Cebral JR. Patient-specific computational fluid dynamics modeling of anterior communicating artery aneurysms: a study of the sensitivity of intra-aneurysmal flow patterns to flow conditions in the carotid arteries. *AJNR Am J Neuroradiol*. 2006;27:2061-2068.

22. Schirmer CM, Malek AM. Wall shear stress gradient analysis within an idealized stenosis using non-Newtonian flow. *Neurosurgery*. 2007;61:853-863. ; discussion 863-4.

23. Zhang J, Can A, Lai PMR, et al. Vascular geometry associated with anterior communicating artery aneurysm formation. *World Neurosurg*. 2021;146:e1318-e1325.

24. de Gast AN, van Rooij WJ, Sluzewski M. Fenestrations of the anterior communicating artery: incidence on 3D angiography and relationship to aneurysms. *Am J Neuroradiol*. 2008;29:296-298.

25. Malek AM, Hippelheuser JE, Lauric A. Vortex formation and associated aneurysmogenic transverse rotational shear stress near the apex of wide-angle cerebral bifurcations. *J Neurosurg*. 2022;136:1726-1737.

26. Juvela S, Porras M, Heiskanen O. Natural history of unruptured intracranial aneurysms: a long-term follow-up study. *J Neurosurg*. 1993;79:174-182.

27. Wiebers DO, Whisnant JP, O'Fallon WM. The natural history of unruptured intracranial aneurysms. *N Engl J Med*. 1981;304:696-698.

28. Juvela SPM, Poussa K. Natural history of unruptured intracranial aneurysms: probability of and risk factors for aneurysm rupture. *J Neurosurg*. 2008;108:1052-1060.

29. Rau T, He X, Venugopal P, et al. Hemodynamic effect of unequal anterior cerebral artery flow rates on the anterior communicating artery bifurcation: a computational fluid dynamics study. *Model Simulat Eng*. 2008;9:691982.

30. Baharoglu MI, Lauric A, Wu C, Hippelheuser J, Malek AM. Deviation from optimal vascular caliber control at middle cerebral artery bifurcations harboring aneurysms. *J Biomech*. 2014;47:3318-3324.

31. Cebral JR, Mut F, Weir J, Putman CM. Association of hemodynamic characteristics and cerebral aneurysm rupture. *AJNR Am J Neuroradiol*. 2011;32:264-270.

32. Canham PB, Finlay HM. Morphometry of medial gaps of human brain artery branches. *Stroke*. 2004;35:1153-1157.

33. Rowe AJ, Finlay HM, Canham PB. Collagen biomechanics in cerebral arteries and bifurcations assessed by polarizing microscopy. *J Vasc Res*. 2003;40:406-415.

34. Meng H, Wang Z, Hoi Y, et al. Complex hemodynamics at the apex of an arterial bifurcation induces vascular remodeling resembling cerebral aneurysm initiation. *Stroke*. 2007;38:1924-1931.

35. Bor AS, Velthuis BK, Majoie CB, Rinkel GJ. Configuration of intracranial arteries and development of aneurysms: a follow-up study. *Neurology*. 2008;70:700-705.

IRB approval: This research was approved by Tufts Health Sciences Campus Institutional Review Board (IRB# 9035). Patient consent was waived because of the retrospective nature of the study not impacting patient clinical care.

Conflict of interest statement: The authors declare that the article content was composed in the absence of any commercial or financial relationships that could be construed as a potential conflict of interest.

Received 29 July 2025; accepted 31 July 2025

Citation: World Neurosurg. (2025) 202:124359. http://doi.org/10.1016/j.wneu.2025.124359

Journal homepage: ***www.journals.elsevier.com/world-neurosurgery***

Available online: ***www.sciencedirect.com***

1878-8750/© 2025 The Author(s). Published by Elsevier Inc. This is an open access article under the CC BY license (http://creativecommons.org/licenses/by/4.0/).